3D MRI of the Shoulder

Steven P. Daniels, MD[1] Soterios Gyftopoulos, MD, MSc[1]

[1] Department of Radiology, New York University Grossman School of Medicine, New York University, New York, New York

Semin Musculoskelet Radiol 2021;25:480–487.

Address for correspondence Soterios Gyftopoulos, MD, MSc, Department of Radiology, New York University Grossman School of Medicine, 660 First Avenue, New York, NY 10016 (e-mail: Soterios.Gyftopoulos@nyumc.org).

Abstract

Magnetic resonance imaging provides a comprehensive evaluation of the shoulder including the rotator cuff muscles and tendons, glenoid labrum, long head biceps tendon, and glenohumeral and acromioclavicular joint articulations. Most institutions use two-dimensional sequences acquired in all three imaging planes to accurately evaluate the many important structures of the shoulder. Recently, the addition of three-dimensional (3D) acquisitions with 3D reconstructions has become clinically feasible and helped improve our understanding of several important pathologic conditions, allowing us to provide added value for referring clinicians. This article briefly describes techniques used in 3D imaging of the shoulder and discusses applications of these techniques including measuring glenoid bone loss in anterior glenohumeral instability. We also review the literature on routine 3D imaging for the evaluation of common shoulder abnormalities as 3D imaging will likely become more common as imaging software continues to improve.

Keywords
- shoulder
- 3D MRI
- glenoid bone loss
- anterior glenohumeral instability

Magnetic resonance imaging (MRI) of the shoulder is one of the most commonly performed examinations in musculoskeletal radiology practice because it provides a comprehensive evaluation of commonly injured structures such as the rotator cuff, glenoid labrum, long head biceps tendon, and glenohumeral and acromioclavicular articulations.[1] Most institutions use two-dimensional (2D) fast spin-echo (FSE) or turbo spin-echo acquisitions in all three imaging planes to accurately evaluate commonly injured structures.[2,3] Three-dimensional (3D) acquisitions provide several potential advantages over 2D acquisitions including the ability to create multiplanar reconstructions for evaluating structures best assessed on nonorthogonal imaging planes and the ability to create 3D models for preoperative planning.[4,5] This technique also has the potential to reduce imaging times significantly without sacrificing diagnostic accuracy in the evaluation of several intra-articular and periarticular structures.[6,7]

This article describes the current use of 3D imaging in the evaluation of the shoulder. We briefly discuss imaging techniques and focus on current clinical applications such as the measurement of glenoid bone loss in cases of anterior glenohumeral instability and the 3D modeling of rotator cuff tears in preoperative planning. Although not currently performed at many institutions, we also briefly review the literature on 3D imaging in the evaluation of commonly injured structures about the shoulder.

Imaging Techniques

Many institutions use 3D acquisitions as an addition to standard protocols rather than as a replacement for 2D acquisitions.[8,9] The most commonly added 3D acquisition is an axial 3D T1 gradient-echo fast low angle shot (FLASH) sequence with two-point Dixon water-fat separation or an axial 3D T1 gradient-echo volume interpolated breath-hold examination (VIBE) with a water excitation sequence, both of which can be used for creating 3D reconstructions of osseous structures.[10–12] VIBE and FLASH are both spoiled gradient-echo (GRE) sequences with similar acquisition times. ►**Table 1** lists the scan parameters for the VIBE sequence commonly used at our institution. Both sequences use the Dixon technique that allows for image postprocessing to accentuate signal from the fat-containing structures and minimize signal from the soft tissue structures. This is performed by using the water-only images and calculating the lowest mean signal intensity from multiple regions of interest placed on the soft tissues surrounding the

Issue Theme 3D MRI of the Musculoskeletal System; Guest Editor, Jan Fritz, MD

Thieme Medical Publishers, Inc., 333 Seventh Avenue, 18th Floor, New York, NY 10001, USA

DOI https://doi.org/10.1055/s-0041-1728813.
ISSN 1089-7860.

Table 1 Scan parameters for axial three-dimensional T1 gradient-echo VIBE sequence with water excitation

Parameter	Value
TR, ms	10
TE, ms	2.46–3.69
Flip angle, degrees	9
FOV, mm	$190 \times 192 \times 120$
Matrix	192×192
Voxel size, mm	$1.0 \times 1.0 \times 1.0$
Acceleration factor	2
Acquisition time	1 min, 10 s

Abbreviations: FOV, field of view; TE, time to echo; TR, repetition time; VIBE, volumetric interpolated breath-hold examination.

osseous structures. The pixel values are then subtracted from this value, and negative values are set to zero, accentuating the signal arising from fat-containing structures such as the bone marrow. Manual segmentation can then be performed to create 3D reconstructions of the osseous anatomy. The total postprocessing time often takes 6 to 7 minutes, allowing for integration into clinical practice.[9] Although VIBE and FLASH were both shown to create accurate reformats, one study comparing the two sequences showed fewer truncation and pulsation artifacts with VIBE.[13]

In addition to being used to create 3D reconstructions of osseous structures, 3D GRE sequences with two-point Dixon water-fat separation, including VIBE, have been used to calculate rotator cuff muscle fat fraction.[14–17] The fat fraction can be calculated by dividing the muscle signal intensity on the fat-only image by the signal intensity on the in-phase image (water only plus fat only). Previous studies acquired these sequences in the sagittal plane for assessment of fat fraction with a scan time as low as 2 minutes and 30 seconds.[18] Unfortunately, the time-consuming nature of muscle segmentation has limited the clinical applicability of this technique. The 3D GRE sequences were also used with chemical fat suppression to evaluate the rotator cuff and labrum after MR arthrography.[6,19,20]

The 3D reconstruction of soft tissue structures around the shoulder, such as the rotator cuff tendons, is difficult to perform. However, images from routine 2D MR acquisitions can be manually segmented to create 3D reconstructions and better delineate soft tissue anatomy, as has been performed to assess the shape of a rotator cuff tear.[21] This process involves manually outlining different points of the rotator cuff tendons from the insertional fibers to the myotendinous junction and connecting the outlines through automatic interpolation. The authors in one study where this was performed noted a postprocessing time between 2 and 3 minutes for each reconstruction.[21]

Recent technological advances, such as parallel imaging and compressed sensing, have allowed for the acquisition of 3D FSE sequences in clinically acceptable scan times.[22–24] Currently, all major vendors offer 3D FSE sequences that can be performed with any desired image-weighting and with or without arthrography.[24–27] Although these sequences have shown promising results in evaluating the shoulder, adaption into routine clinical practice has been slow. This is likely due to the relatively long acquisition time, often between 7 and 8 minutes at 1.5 T for the shoulder, which makes these sequences susceptible to patient motion and difficult to repeat, if necessary, while remaining within a scheduled time slot.[27,28] Imaging at 3 T has the potential to shorten sequence acquisition times, although published acquisition times are still between 6 and 8 minutes.[22,25,26] Another commonly cited concern with using 3D acquisitions is image blurring, causing structural edges to become indistinct.[29] Newer imaging techniques, such as controlled aliasing in parallel imaging results in higher acceleration (CAIPIRINHA), may help overcome some of these difficulties, but data are limited on its use in the shoulder.[30]

Clinical Applications

Anterior Glenohumeral Instability

Anterior dislocation of the glenohumeral joint is a common injury, with dislocations occurring most often in men between 15 and 29 years of age while participating in sports.[31] Anterior dislocation is a significant injury with the potential to disrupt several structures including the glenoid labrum, articular cartilage, joint capsule, anterior glenoid periosteum, biceps tendon, and rotator cuff tendons. Anterior glenohumeral dislocation also causes impaction of the posterior humeral head (Hill-Sachs lesion) in most patients and a glenoid rim fracture (osseous Bankart lesion) in just over 20% of patients after first-time traumatic dislocation.[32] Glenoid bone loss, which can be due to either an osseous Bankart lesion or chronic impaction and attritional change, is thought to occur in $>90\%$ of patients with recurrent anterior glenohumeral instability and is a predictor of future instability events after soft tissue Bankart repair.[33] Biomechanical cadaveric studies show that the extent of both Hill-Sachs lesions and glenoid bone loss contribute to glenohumeral instability.[34]

The treatment of anterior glenohumeral instability is complex and depends on both patient factors and the extent of injury.[35] Specifically, in young, active patients, the extent of the Hill-Sachs lesion and the degree of glenoid bone loss dictate whether the patient will need an additional procedure to be performed along with a soft tissue Bankart repair.[36] Biomechanical studies demonstrate decreased joint stability in shoulders with glenoid bone loss $\geq$ 19% after soft tissue Bankart repair, so many surgeons use 20% as a cut-off for the requirement of a glenoid augmentation procedure, such as an iliac crest bone graft or Latarjet procedure.[35–37] But data indicate that outcomes are worse in active, younger patients with as little as 12 to 15% glenoid bone loss, and the presence and size of a concomitant Hill-Sachs lesion is thought to be a key factor in patient outcomes.[36,38,39] Therefore, accurate preoperative delineation of the osseous anatomy is vital for surgical planning and setting patient expectations.

MRI is the most accurate test for evaluating the extent of soft tissue injury after glenohumeral dislocation. Previous research showed 3D computed tomography (CT) to be the

most accurate method for measuring glenoid bone loss, so traditional practice guidelines recommend 3D CT in patients with osseous injury identified at MRI or on initial radiographs.[40] Although CT has superior bony detail when compared with MRI, the examination comes with added cost, exposes patients to radiation, and often requires an additional appointment at the imaging facility, which can be inconvenient. The recent ability to perform 3D GRE sequences in an acceptable time frame and use image postprocessing to create 3D reformats of osseous structures has obviated the need to obtain CTs routinely at many institutions.[9,10,12]

The use of 3D GRE sequences to create 3D reformats of the glenoid was first demonstrated in 2013 in a pilot study that compared 3D MRI with 3D CT and digital photographs of seven cadaveric specimens.[10] That study showed 3D MRI to be accurate when compared with 3D CT for numerous anatomical measurements and accurate when compared with 3D CT and digital photographs in quantifying glenoid bone loss. A follow-up 2014 article by the same group demonstrated 3D MRI to be accurate in quantifying glenoid bone loss in 15 patients when compared with arthroscopic assessment using the bare spot method.[9] Importantly, this article showed the true mean absolute error of 3D MRI to be $< 2.2\%$ when compared with arthroscopic assessment and showed 3D MRI to be accurate in postoperative patients and in arthrographic and non-arthrographic MRI studies. Studies by other groups with similar imaging techniques yielded comparable results, suggesting this is a generalizable technique.[11,12,41,42]

The 3D reformats of the glenoid with the humerus subtracted allow for an accurate en face assessment of the glenoid articular surface to calculate glenoid bone loss. The best fit circle methods were shown to be accurate and reproducible and are commonly performed at our institution (►**Fig. 1**).[43] First, a line is drawn from the supraglenoid tubercle through the inferior glenoid rim along the long axis of the glenoid. Next,

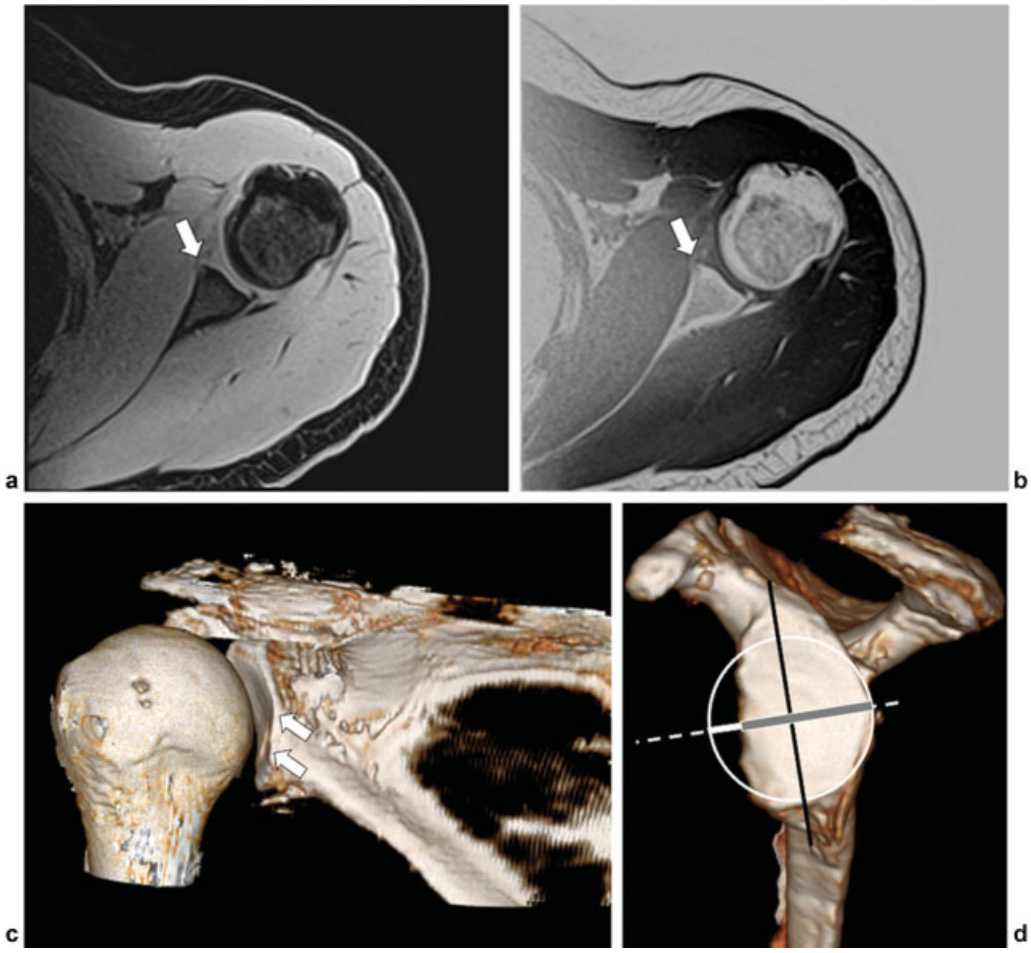

Fig. 1 A 19-year-old man with multiple prior anterior glenohumeral dislocations. (**a**) Axial water-only MR image and (**b**) corresponding subtraction image demonstrate flattening of the anterior glenoid due to chronic attrition from multiple prior dislocations (white arrow). The subtraction image accentuates signal in the osseous structures. (**c**) Three-dimensional (3D) reconstruction of the humerus and scapula demonstrate flattening of the anterior glenoid (white arrows) (**d**) 3D reconstruction of the scapula with the humerus subtracted allows for an en face view of the glenoid to calculate glenoid bone loss. First, a line is drawn through the long axis of the glenoid (black line) passing through the supraglenoid tubercle. Next, a best fit circle is drawn and lined up with the intact posterior inferior glenoid (white circle). A line through the short axis of the glenoid is then drawn (dashed white line), ensuring it crosses through the center of the best fit circle. This allows for measurement of the residual glenoid width (gray line) and size of the anterior glenoid osseous defect (solid white line). The percentage of glenoid bone loss can be calculated as the size of the anterior glenoid osseous defect divided by the estimated intact glenoid diameter (anterior glenoid osseous defect plus residual glenoid width).

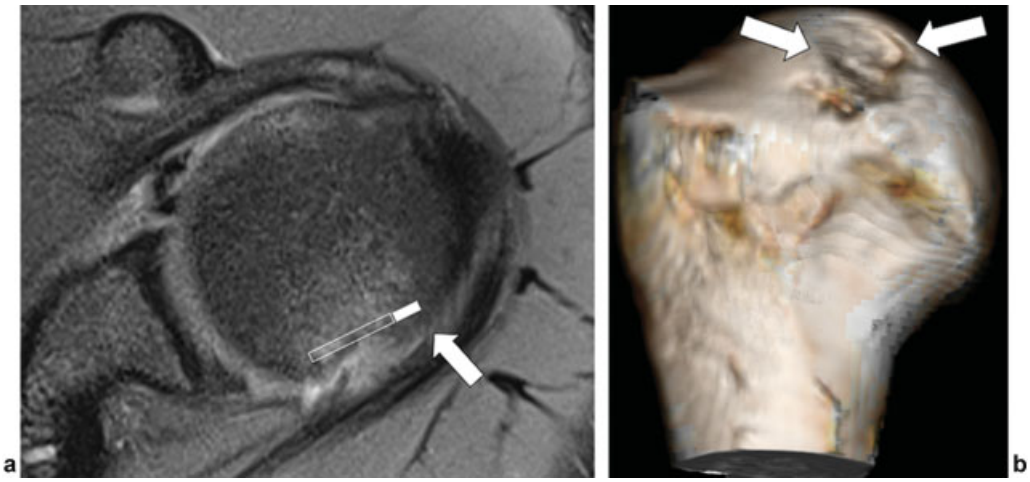

Fig. 2 A 24-year-old man with anterior glenohumeral instability. (**a**) Axial proton-density fat-suppressed MR image demonstrates an acute Hill-Sachs lesion (outlined white rectangle). Measurement of the Hill-Sachs interval includes the Hill-Sachs lesion as well as the bony bridge (solid white rectangle) between the lateral aspect of the lesion and the rotator cuff insertion (white arrow). (**b**) Three-dimensional reformat of the humerus demonstrates the Hill-Sachs lesion (white arrows).

a best fit circle is placed about the intact portions of the posterior and inferior glenoid and increased in size to approximate the glenoid articular surface. A transverse line is drawn through the center of the circle, perpendicular to the vertical line representing the long axis of the glenoid, to estimate the anterior to posterior diameter of the intact glenoid and the width of the area of glenoid bone loss. The percentage of glenoid bone loss can then be calculated as the estimated width of defect divided by the estimated diameter of intact glenoid.

The Hill-Sachs interval can be measured on axial sequences as the width of the Hill-Sachs lesion in millimeters plus the width of the osseous bridge between the lateral margin of the Hill-Sachs lesion and the medial aspect of the rotator cuff attachment (►**Fig. 2**). The interaction between glenoid bone loss and the Hill-Sachs interval can be demonstrated in the concept of the glenoid track that describes the zone of contact between the humeral head and the glenoid.[44] The glenoid track is ~ 83% of the estimated intact glenoid width minus the amount of anterior glenoid bone loss (►**Fig. 3**). In cases where the Hill-Sachs interval exceeds the glenoid track, the lesion is thought to be "off track" and at risk for engagement after a soft tissue Bankart repair.[36,45] If the Hill-Sachs interval is less than the glenoid track, the lesion is thought to be "on track" and not at risk for engagement after a soft tissue Bankart repair. A 2015 study with 76 patients showed MRI to be 84.5% accurate in evaluating on-track versus off-track status with a sensitivity of 72.2% and specificity of 87.9% in identifying off-track lesions.[46]

Shoulder Arthroplasty

Glenohumeral osteoarthritis is common and often treated with either reverse or anatomical total shoulder arthroplasty. In the preoperative evaluation of arthroplasty candidates, an accurate assessment of glenoid morphology is essential to increase the chances of a successful long-term outcome and minimize the risk of complications such as glenoid component loosening.[47] Features traditionally assessed using 3D CT include glenoid version, glenoid bone loss, and Walch glenoid classification.[48]

The key to making these measurements accurately is using axial images in the plane of the scapula that is often oblique to the axial, sagittal, and coronal imaging planes and easier to obtain with a 3D data set. These measurements can also be obtained accurately using 3D MRI reformats, and MRI provides the added benefit of simultaneous accurate evaluation of the rotator cuff musculature and tendon quality.[48] Status of the rotator cuff is a key deciding factor in whether patients will undergo reverse or anatomical total shoulder arthroplasty.[49] Further research is necessary to demonstrate the ability of 3D MRI to evaluate glenoid morphology accurately as this could save patients from having an additional CT if they are already undergoing an MRI to evaluate the rotator cuff.

Rotator Cuff Tears

Rotator cuff tears are a common cause of pain and disability, and a suspected rotator cuff tear is a frequent indication for MRI of the shoulder. MRI is a very accurate test for identifying rotator cuff tears. Tear size, tendon retraction, and tendon degeneration were shown to correlate with worse clinical outcomes after rotator cuff repair.[2,50] Accurate preoperative imaging characterization of a rotator cuff tear provides valuable prognostic information for the treating surgeon. 3D FSE sequences have demonstrated similar performance to 2D sequences in identifying rotator cuff tears in non-arthrographic MRIs.[26,51]

As mentioned previously, 3D sequences have the added benefit of the ability to be reformatted in nonstandard imaging planes, including into an angled oblique sagittal plane oriented perpendicular to the distal supraspinatus tendon. This plane was shown to be helpful in identifying distal partial-thickness rotator cuff tears and is commonly performed at some institutions.[52,53] A 2018 study comparing 3D FSE and 2D FSE sequences in 74 patients with arthroscopic correlation showed 3D sequences to be 95% sensitive, 100% specific, and 95%

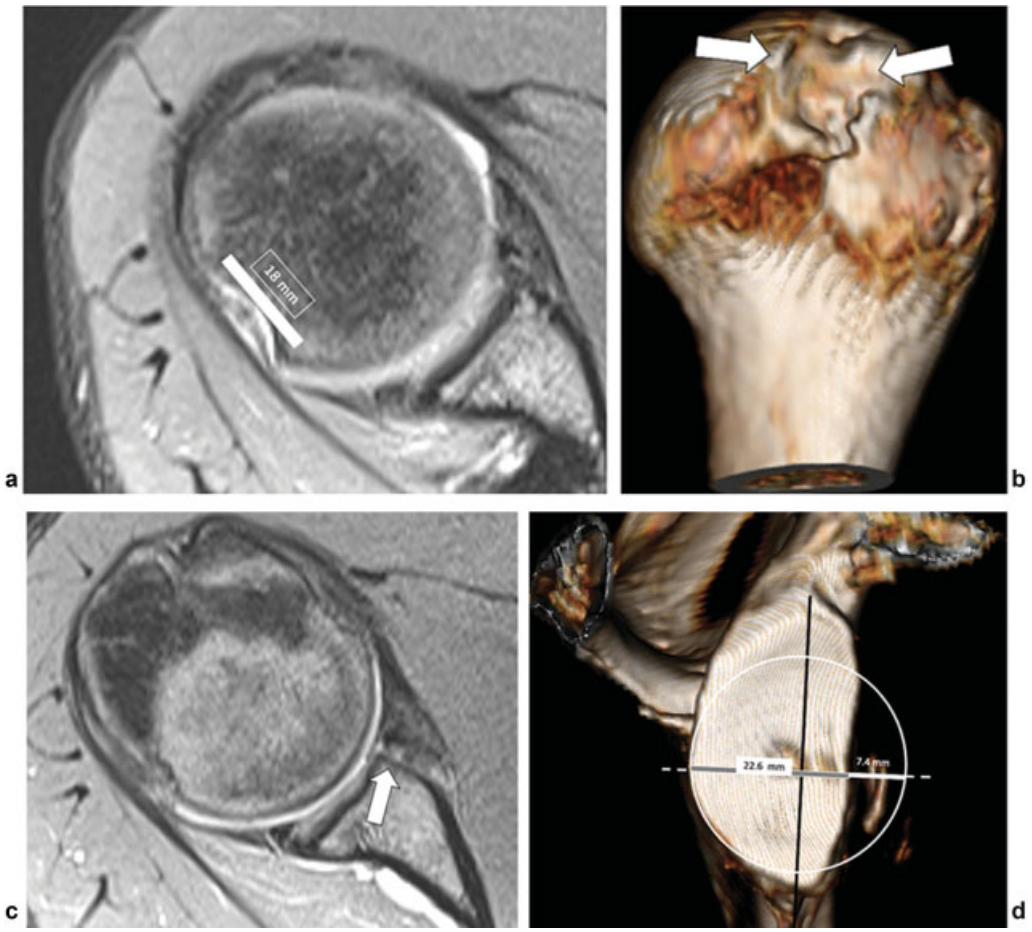

Fig. 3 A 17-year-old young man with repeated anterior glenohumeral dislocations after a skateboarding injury 1 year earlier. (**a**) Axial proton-density fat-suppressed MR image demonstrates a Hill-Sachs lesion with a Hill-Sachs interval of 18 mm. (**b**) Three-dimensional (3D) reconstruction of the humerus demonstrates the extent of the Hill-Sachs lesion (white arrows). (**c**) A more inferior axial proton-density fat-suppressed MR image demonstrates anterior glenoid bone loss (white arrow). (**d**) 3D reconstruction of the scapula with en face view of the glenoid demonstrates 7.4-mm of anterior glenoid bone loss (white line) with residual glenoid width of 22.6 mm (gray line). Glenoid bone loss was calculated as 25%: 7.4 mm/(22.6 mm + 7.4 mm). Also, the Hill-Sachs interval (18 mm) was greater than the glenoid track (0.83 × 30.0 mm – 7.4 mm = 17.5 mm), consistent with an off-track lesion. The patient was treated with the Latarjet procedure. Black line in (d) indicates long axis of the glenoid; dashed white line in (d) indicates the short axis of the glenoid.

accurate in identifying supraspinatus-infraspinatus tendon tears compared with 99%, 93%, and 98% on 2D sequences.[26] However, that same study showed 3D FSE to be slightly less reliable and less specific in identifying subscapularis tears, which was thought to be due to blurring and motion. Correlation of imaging and arthroscopic evaluation of the subscapularis tendon is difficult because the middle to distal tendon footprints are challenging to evaluate arthroscopically without a dedicated evaluation and a high suspicion for pathology.[54]

Multiple studies have compared 3D MR arthrograms with 2D MR arthrograms in evaluation of the rotator cuff. A meta-analysis in 2018 showed 3D MR arthrography to have a sensitivity of 91% and a specificity of 90% in identifying rotator cuff tears compared with 92% and 90%, respectively, for conventional 2D MR arthrography. It also showed 3D-FSE sequences to have a higher sensitivity compared with 3D GRE sequences.[55] However, 3D GRE sequences such as VIBE can be obtained very quickly and demonstrate good concordance with 2D sequences and arthroscopic evaluation.[19]

The size and shape of rotator cuff tears play an important role in surgical management. A 2016 study showed manually segmented 3D MRI reconstructions to be more accurate than 2D MR sequences in characterizing the shape of rotator cuff tears.[21] These tears are commonly described as crescent shaped, with greater width (anteroposterior dimension) than length (mediolateral dimension), or longitudinal, with greater length than width. Longitudinal tears are often divided into U-shaped tears, with intact anterior supraspinatus and posterior infraspinatus tendon tissue, and L-shaped tears that involve the anterior supraspinatus tendon fibers and extend into the rotator interval. The 3D MRI reconstructions were 82% accurate when characterizing tears as U shaped, L shaped, or crescent shaped, versus 64.7% when using only 2D sequences (►**Fig. 4**). Longitudinal tears differ from crescent-shaped tears because they may require side-to-side closure before direct attachment to the greater tuberosity to ensure a stable repair.[56] The 3D reconstructions allow for improved visualization and conceptualization of this complex anatomy. Thus 3D

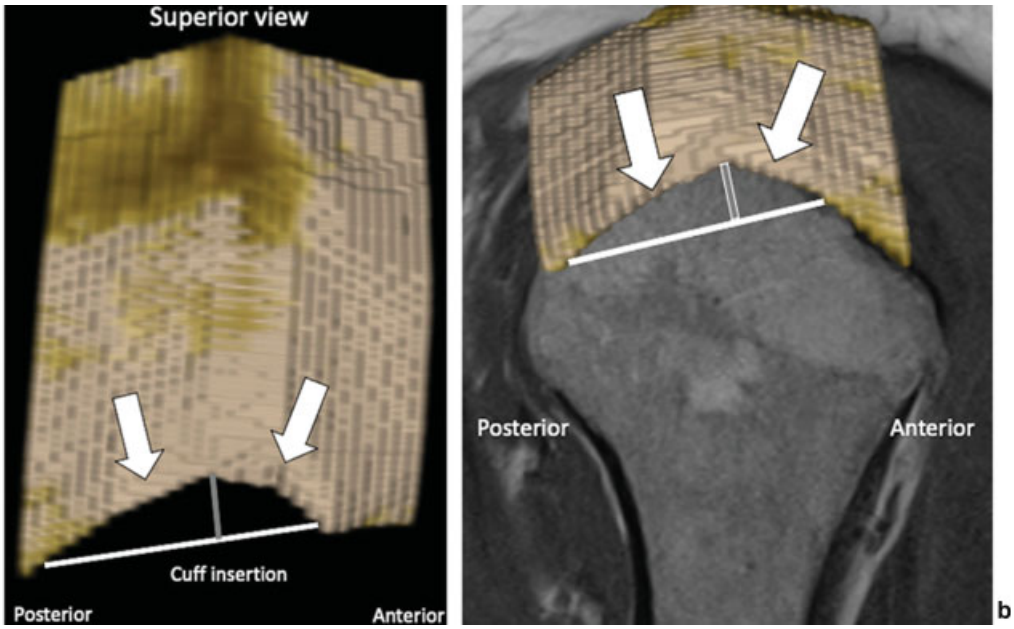

Fig. 4 Three-dimensional (3D) reconstruction to demonstrate rotator cuff tear shape. (**a**) Superior view of the 3D reconstruction of the rotator cuff demonstrates a crescent-shaped tear (white arrows) with the width (white line) greater than the length (gray line). (**b**) The 3D reconstruction superimposed on a sagittal MR image demonstrates tear morphology in relation to the humeral head.

sequence acquisitions will ideally allow for improved 3D reformats of soft tissue structures to improve characterization of rotator cuff tear shape, although to our knowledge, this has not been studied.

Along with identifying and characterizing rotator cuff tendon pathology, MRI has the added benefit of allowing for accurate evaluation of the muscle including muscle bulk and fatty infiltration.[57] Fatty infiltration of the rotator cuff muscles is a known negative prognostic factor in patients who undergo rotator cuff repair.[2] As such, accurate assessment of rotator cuff fatty infiltration helps surgeons establish a treatment strategy and discuss the prognosis with patients.

Rotator cuff muscle bulk and fatty infiltration are traditionally evaluated with the Thomazeau and Goutallier classifications, respectively.[58,59] The Thomazeau classification evaluates the portion of the supraspinatus fossa occupied by the muscle belly, termed the *occupation ratio.* It is calculated by dividing the surface area of the supraspinatus muscle belly by that of the entire supraspinatus fossa on the sagittal oblique image at the medial border of the scapular spine above the spinoglenoid notch. A ratio of 0.6 to 1.0 indicates normal bulk or slight atrophy, 0.4 to 0.6 indicates moderate atrophy, and < 0.4 represents severe atrophy.[58] The Goutallier classification is from 0 to 4 with grade 0 representing normal muscle; grade 1, fatty streaks within the muscle belly; grade 2, $< 50\%$ fatty infiltration; grade 3, 50% fatty infiltration; and grade 4, $> 50\%$ fatty infiltration. The Goutallier classification is subject to a high degree of intraobserver and interobserver variability.[60] Due to the subjectivity and variability with the Goutallier classification, there is interest in quantitative methods for evaluating rotator cuff muscle fatty infiltration.

Multiple studies have used 3D GRE acquisitions with Dixon fat and water separation to calculate rotator cuff muscle fat fraction, and have shown muscle fat fraction to be more reliable than the Goutallier classification.[18] Fat fraction correlated with shoulder pain and decreased range of motion as well as tendon tear severity and muscle atrophy.[14,16,17] Fat fraction also correlated with an increased risk of tendon re-tear in patients with full-thickness supraspinatus tears who undergo repair.[61] Although traditionally calculated in the sagittal plane, 3D acquisition allows for assessment of the rotator cuff muscle in any plane, which may be helpful in the setting of a retracted rotator cuff tear.[62]

Labral Tears and Cartilage

Along with rotator cuff tears, labral tears are also a common cause of pain and a reason for referral for MRI of the shoulder. Multiple studies showed 3D MR arthrography using both GRE and FSE sequences to have similar sensitivity and specificity in identifying labral tears when compared with 2D MR arthrography.[6,25,55] The 3D imaging allows for a single acquisition and can obviate the need to perform three planes of traditional T1 fat-suppressed sequences, thus shortening examination time. In a recent meta-analysis from 2018, which included five studies that used FSE sequences and six studies that used GRE sequences, 3D MR arthrography had a pooled sensitivity of 89% and pooled specificity of 95% in identifying labral lesions, which was not significantly different from the findings of 2D MR arthrography.[55] The 3D FSE sequences are a better option in postoperative patients because they demonstrate less artifact around surgical materials.

Unlike in the knee, there is very little research on accuracy of 3D MRI in evaluating cartilage of the glenohumeral joint.[29,63] A 2012 study showed 3D FSE sequences to have decreased sensitivity for partial-thickness articular cartilage lesions of the glenoid when compared with 2D acquisitions, which the authors attributed to increased blurring.[27] Further research is necessary to evaluate newer 3D imaging techniques

that now are shown to have similar accuracy to that of 2D acquisitions in evaluating cartilage of the knee joint.[63]

Conclusion

MRI of the shoulder is commonly performed to evaluate shoulder pain. The recent improvements in 3D acquisitions have allowed these sequences to be obtained in clinically feasible scan times. They allow 3D reconstructions to highlight certain pathologic conditions, such as glenoid bone loss in anterior glenohumeral instability, and to calculate rotator cuff muscle fat fraction, which has prognostic significance in the setting of a rotator cuff tear. As imaging software continues to improve, 3D imaging will likely replace 2D imaging for several MRI indications, allowing for customized imaging planes and decreased examination times.

Conflict of Interest
None declared.

References

1 Tuite MJ, Small KM. Imaging evaluation of nonacute shoulder pain. AJR Am J Roentgenol 2017;209(03):525–533
2 Kijowski R, Thurlow P, Blankenbaker D, et al. Preoperative MRI shoulder findings associated with clinical outcome 1 year after rotator cuff repair. Radiology 2019;291(03):722–729
3 Gottsegen CJ, Merkle AN, Bencardino JT, Gyftopoulos S. Advanced MRI techniques of the shoulder joint: current applications in clinical practice. AJR Am J Roentgenol 2017;209(03):544–551
4 Altahawi F, Subhas N. 3D MRI in musculoskeletal imaging: current and future applications. Curr Radiol Rep 2018;6(08):
5 Naraghi A, White LM. Three-dimensional MRI of the musculoskeletal system. AJR Am J Roentgenol 2012;199(03):W283–W293
6 Jung JY, Yoon YC, Choi SH, Kwon JW, Yoo J, Choe BK. Three-dimensional isotropic shoulder MR arthrography: comparison with two-dimensional MR arthrography for the diagnosis of labral lesions at 3.0 T. Radiology 2009;250(02):498–505
7 Fritz J, Ahlawat S, Fritz B, et al. 10-min 3D turbo spin echo MRI of the knee in children: arthroscopy-validated accuracy for the diagnosis of internal derangement. J Magn Reson Imaging 2019;49(07):e139–e151
8 Kijowski R, Blankenbaker DG, Woods M, Del Rio AM, De Smet AA, Reeder SB. Clinical usefulness of adding 3D cartilage imaging sequences to a routine knee MR protocol. AJR Am J Roentgenol 2011;196(01):159–167
9 Gyftopoulos S, Beltran LS, Yemin A, et al. Use of 3D MR reconstructions in the evaluation of glenoid bone loss: a clinical study. Skeletal Radiol 2014;43(02):213–218
10 Gyftopoulos S, Yemin A, Mulholland T, et al. 3DMR osseous reconstructions of the shoulder using a gradient-echo based two-point Dixon reconstruction: a feasibility study. Skeletal Radiol 2013;42(03):347–352
11 Yanke AB, Shin JJ, Pearson I, et al. Three-dimensional magnetic resonance imaging quantification of glenoid bone loss is equivalent to 3-dimensional computed tomography quantification: cadaveric study. Arthroscopy 2017;33(04):709–715
12 Lansdown DA, Cvetanovich GL, Verma NN, et al. Automated 3-dimensional magnetic resonance imaging allows for accurate evaluation of glenoid bone loss compared with 3-dimensional computed tomography. Arthroscopy 2019;35(03):734–740
13 Zheng Z-Z, Shan H, Li X. Fat-suppressed 3D T1-weighted gradient-echo imaging of the cartilage with a volumetric interpolated breath-hold examination. AJR Am J Roentgenol 2010;194(05):W414–W419
14 Nardo L, Karampinos DC, Lansdown DA, et al. Quantitative assessment of fat infiltration in the rotator cuff muscles using water-fat MRI. J Magn Reson Imaging 2014;39(05):1178–1185
15 Lee YH, Kim S, Lim D, Song H-T, Suh J-S. MR quantification of the fatty fraction from T2*-corrected Dixon fat/water separation volume-interpolated breathhold examination (VIBE) in the assessment of muscle atrophy in rotator cuff tears. Acad Radiol 2015;22(07):909–917
16 Lee S, Lucas RM, Lansdown DA, et al. Magnetic resonance rotator cuff fat fraction and its relationship with tendon tear severity and subject characteristics. J Shoulder Elbow Surg 2015;24(09):1442–1451
17 Nozaki T, Tasaki A, Horiuchi S, et al. Quantification of fatty degeneration within the supraspinatus muscle by using a 2-point Dixon method on 3-T MRI. AJR Am J Roentgenol 2015;205(01):116–122
18 Horiuchi S, Nozaki T, Tasaki A, et al. Reliability of MR quantification of rotator cuff muscle fatty degeneration using a 2-point Dixon technique in comparison with the Goutallier classification: validation study by multiple readers. Acad Radiol 2017;24(11):1343–1351
19 Vandevenne JE, Vanhoenacker F, Mahachie John JM, Gelin G, Parizel PM. Fast MR arthrography using VIBE sequences to evaluate the rotator cuff. Skeletal Radiol 2009;38(07):669–674
20 Lee SH, Yun SJ, Yoon Y. Diagnostic performance of shoulder magnetic resonance arthrography for labral tears having surgery as reference: comparison of high-resolution isotropic 3D sequence (THRIVE) with standard protocol. Radiol Med (Torino) 2018;123(08):620–630
21 Gyftopoulos S, Beltran LS, Gibbs K, et al. Rotator cuff tear shape characterization: a comparison of two-dimensional imaging and three-dimensional magnetic resonance reconstructions. J Shoulder Elbow Surg 2016;25(01):22–30
22 Lee SH, Lee YH, Song H-T, Suh J-S. Rapid acquisition of magnetic resonance imaging of the shoulder using three-dimensional fast spin echo sequence with compressed sensing. Magn Reson Imaging 2017;42:152–157
23 Kijowski R, Rosas H, Samsonov A, King K, Peters R, Liu F. Knee imaging: rapid three-dimensional fast spin-echo using compressed sensing. J Magn Reson Imaging 2017;45(06):1712–1722
24 Li CQ, Chen W, Rosenberg JK, et al. Optimizing isotropic three-dimensional fast spin-echo methods for imaging the knee. J Magn Reson Imaging 2014;39(06):1417–1425
25 Choo HJ, Lee SJ, Kim O-H, Seo SS, Kim JH. Comparison of three-dimensional isotropic T1-weighted fast spin-echo MR arthrography with two-dimensional MR arthrography of the shoulder. Radiology 2012;262(03):921–931
26 Hong WS, Jee WH, Lee SY, Chun CW, Jung JY, Kim YS. Diagnosis of rotator cuff tears with non-arthrographic MR imaging: 3D fat-suppressed isotropic intermediate-weighted turbo spin-echo sequence versus conventional 2D sequences at 3T. Investig Magn Reson Imaging 2018;22(04):229–239
27 Rybak LD, La Rocca Vieira R, Recht M, et al. Preliminary study of 1.5-T MR arthrography of the shoulder with 3D isotropic intermediate-weighted turbo spin echo. AJR Am J Roentgenol 2012;199(01):W107–W113
28 Glaser C, D'Anastasi M, Theisen D, et al. Understanding 3D TSE sequences: advantages, disadvantages, and application in MSK imaging. Semin Musculoskelet Radiol 2015;19(04):321–327
29 Kijowski R, Gold GE. Routine 3D magnetic resonance imaging of joints. J Magn Reson Imaging 2011;33(04):758–771
30 Del Grande F, Delcogliano M, Guglielmi R, et al. Fully automated 10-minute 3D CAIPIRINHA SPACE TSE MRI of the knee in adults: a multicenter, multireader, multifield-strength validation study. Invest Radiol 2018;53(11):689–697
31 Zacchilli MA, Owens BD. Epidemiology of shoulder dislocations presenting to emergency departments in the United States. J Bone Joint Surg Am 2010;92(03):542–549

32 Taylor DC, Arciero RA. Pathologic changes associated with shoulder dislocations. Arthroscopic and physical examination findings in first-time, traumatic anterior dislocations. Am J Sports Med 1997;25(03):306–311

33 Burkhart SS, De Beer JF. Traumatic glenohumeral bone defects and their relationship to failure of arthroscopic Bankart repairs: significance of the inverted-pear glenoid and the humeral engaging Hill-Sachs lesion. Arthroscopy 2000;16(07):677–694

34 Arciero RA, Parrino A, Bernhardson AS, et al. The effect of a combined glenoid and Hill-Sachs defect on glenohumeral stability: a biomechanical cadaveric study using 3-dimensional modeling of 142 patients. Am J Sports Med 2015;43(06):1422–1429

35 Streubel PN, Krych AJ, Simone JP, et al. Anterior glenohumeral instability: a pathology-based surgical treatment strategy. J Am Acad Orthop Surg 2014;22(05):283–294

36 Di Giacomo G, de Gasperis N, Scarso P. Bipolar bone defect in the shoulder anterior dislocation. Knee Surg Sports Traumatol Arthrosc 2016;24(02):479–488

37 Yamamoto N, Muraki T, Sperling JW, et al. Stabilizing mechanism in bone-grafting of a large glenoid defect. J Bone Joint Surg Am 2010;92(11):2059–2066

38 Dekker TJ, Peebles LA, Bernhardson AS, et al. Risk factors for recurrence after arthroscopic instability repair—the importance of glenoid bone loss >15%, patient age, and duration of symptoms: a matched cohort analysis. Am J Sports Med 2020;48(12):3036–3041

39 Shaha JS, Cook JB, Song DJ, et al. Redefining "critical" bone loss in shoulder instability. Am J Sports Med 2015;43(07):1719–1725

40 Bishop JY, Jones GL, Rerko MA, Donaldson CMOON Shoulder Group. 3-D CT is the most reliable imaging modality when quantifying glenoid bone loss. Clin Orthop Relat Res 2013;471 (04):1251–1256

41 Stillwater L, Koenig J, Maycher B, Davidson M. 3D-MR vs. 3D-CT of the shoulder in patients with glenohumeral instability. Skeletal Radiol 2017;46(03):325–331

42 Vopat BG, Cai W, Torriani M, et al. Measurement of glenoid bone loss with 3-dimensional magnetic resonance imaging: a matched computed tomography analysis. Arthroscopy 2018;34(12):3141–3147

43 Walter WR, Samim M, LaPolla FWZ, Gyftopoulos S. Imaging quantification of glenoid bone loss in patients with glenohumeral instability: a systematic review. AJR Am J Roentgenol 2019;212(05):1–10

44 Yamamoto N, Itoi E, Abe H, et al. Contact between the glenoid and the humeral head in abduction, external rotation, and horizontal extension: a new concept of glenoid track. J Shoulder Elbow Surg 2007;16(05):649–656

45 Shaha JS, Cook JB, Rowles DJ, Bottoni CR, Shaha SH, Tokish JM. Clinical validation of the glenoid track concept in anterior glenohumeral instability. J Bone Joint Surg Am 2016;98(22):1918–1923

46 Gyftopoulos S, Beltran LS, Bookman J, Rokito A. MRI evaluation of bipolar bone loss using the on-track off-track method: a feasibility study. AJR Am J Roentgenol 2015;205(04):848–852

47 Strauss EJ, Roche C, Flurin P-H, Wright T, Zuckerman JD. The glenoid in shoulder arthroplasty. J Shoulder Elbow Surg 2009;18 (05):819–833

48 Sharifi A, Siebert MJ, Chhabra A. How to measure glenoid bone stock and version and why it is important: a practical guide. Radiographics 2020;40(06):1671–1683

49 Jarrett CD, Brown BT, Schmidt CC. Reverse shoulder arthroplasty. Orthop Clin North Am 2013;44(03):389–408, x

50 de Jesus JO, Parker L, Frangos AJ, Nazarian LN. Accuracy of MRI, MR arthrography, and ultrasound in the diagnosis of rotator cuff tears: a meta-analysis. AJR Am J Roentgenol 2009;192(06): 1701–1707

51 Kloth JK, Winterstein M, Akbar M, et al. Comparison of 3D turbo spin-echo SPACE sequences with conventional 2D MRI sequences to assess the shoulder joint. Eur J Radiol 2014;83(10):1843–1849

52 Tuite MJ, Asinger D, Orwin JF. Angled oblique sagittal MR imaging of rotator cuff tears: comparison with standard oblique sagittal images. Skeletal Radiol 2001;30(05):262–269

53 Etancelin-Jamet M, Bouilleau L, Martin A, Bertrand P. Diagnostic value of angled oblique sagittal images of the supraspinatus tendon for the detection of rotator cuff tears on MR imaging. Diagn Interv Imaging 2017;98(02):161–169

54 Koo SS, Burkhart SS. Subscapularis tendon tears: identifying mid to distal footprint disruptions. Arthroscopy 2010;26(08):1130–1134

55 Lee SH, Yun SJ, Jin W, Park SY, Park JS, Ryu KN. Comparison between 3D isotropic and 2D conventional MR arthrography for diagnosing rotator cuff tear and labral lesions: a meta-analysis. J Magn Reson Imaging 2018;48(04):1034–1045

56 Burkhart SS. A stepwise approach to arthroscopic rotator cuff repair based on biomechanical principles. Arthroscopy 2000;16 (01):82–90

57 Somerson JS, Hsu JE, Gorbaty JD, Gee AO. Classifications in brief: Goutallier classification of fatty infiltration of the rotator cuff musculature. Clin Orthop Relat Res 2016;474(05):1328–1332

58 Thomazeau H, Rolland Y, Lucas C, Duval JM, Langlais F. Atrophy of the supraspinatus belly. Assessment by MRI in 55 patients with rotator cuff pathology. Acta Orthop Scand 1996;67(03):264–268

59 Goutallier D, Postel J-M, Bernageau J, Lavau L, Voisin M-C. Fatty muscle degeneration in cuff ruptures. Pre- and postoperative evaluation by CT scan. Clin Orthop Relat Res 1994; (304):78–83

60 Schiefer M, Mendonça R, Magnanini MM, et al. Intraobserver and interobserver agreement of Goutallier classification applied to magnetic resonance images. J Shoulder Elbow Surg 2015;24(08):1314–1321

61 Nozaki T, Tasaki A, Horiuchi S, et al. Predicting retear after repair of full-thickness rotator cuff tear: two-point Dixon MR imaging quantification of fatty muscle degeneration-initial experience with 1-year follow-up. Radiology 2016;280(02):500–509

62 Chitkara M, Albert M, Wong T, O'Donnell J, Gyftopoulos S. Rotator cuff fatty infiltration: are coronal images more helpful for characterization than sagittal images? Bull Hosp Jt Dis (2013) 2016;74 (02):130–134

63 Shakoor D, Guermazi A, Kijowski R, et al. Diagnostic performance of three-dimensional MRI for depicting cartilage defects in the knee: a meta-analysis. Radiology 2018;289(01):71–82